Ravindra Kumar*, V. K. Tewari and Satya Prakash

Oxidation Behaviour of Welded ASTM-SA210 GrA1 Boiler Tube Steels under Cyclic Conditions at 900°C in Air

https://doi.org/10.1515/htmp-2018-0017
Received September 01, 2017; accepted August 12, 2018

Abstract: ASTM-SA210-Grade A1 boiler tube steels were welded by shielded metal arc welding (SMAW) and tungsten inert gas processes. The oxidation behaviour of the welded steels was evaluated under cyclic conditions at 900°C. Visual observations and thermogravimetric data were measured at the end of each cycle. Finally, the scale was analysed using X-ray Diffraction, Scanning-Electron Microscopy/Energy-Dispersive X-Ray studies. A SEM Back scattered image analysis of the cross-section of the oxide scale thickness has been made to measure the oxide scales formed over the welded steels. SMAW welded steel showed the more oxidation rate (in terms of weight gain) as compared to TIG welded at the test temperature of 900°C and it was due to the formation of more cracks in oxide scale, and a thick oxide scale was found on HAZ and weld region.

Keywords: oxidation, GrA1 boiler tube steel, shielded metal arc welding (SMAW), tungsten inert gas (TIG)

Introduction

The Ferritic steels used in wide range of applications in boilers, especially in the construction of their water walls because of their low cost, good mechanical properties and resistance to corrosion at elevated temperature. A large number of welds were found in typical thermal power plants, the weldment specially consists of weld metal and heat-affected zone (HAZ). HAZ is the region of base metal that affected during welding. The welded components of steels suffer deleterious micro- structural degradation, most of the service failures are reported to occur in the HAZs. However, no alloy is perfect to resist the corrosion. Any welding techniques that can reduce or eliminate the corrosion increase the life of welded components and its reliability [1–6]. During the weld thermal cycle, extremely high temperatures are reached within the HAZ and this can cause the carbide distribution to differ significantly from that of the original, unaffected base metal. The initial carbides may coarsen, transform to subsequent carbide species *in situ* or completely dissolve and be replaced by a dispersion of new carbides. The manner in which the carbides are affected depends upon factors such as peak temperature, dwell time and cooling rate. In tungsten inert gas welding process a much narrower HAZ is produced [7]. HAZ is the regions which oxides at much higher rate due to the formation of much more extensive internal oxidation and void formation in the subscale regions than in the subscales of the weld metal and base metal regions [8]. For most of the materials the cyclic testing was performed for 50 cycles as this duration is considered to be adequate to achieve the steady state of oxidation The aim of cyclic loading was to create severe conditions for testing as these conditions constitute more realistic approach towards solving the metal corrosion problem in actual industrial environment [9–12].

This study is an attempt to compare oxidation behaviour of welded Gr A1 boiler tube steels subjected to cyclic conditions in air at 900°C. The X-ray diffraction (XRD) and scanning electron microscopy/energy-dispersive X-ray analysis (SEM/EDX) have been used to characterize the corrosion product after high temperature oxidation at 900°C.

Experimental procedures

Selection of materials and preparation of weldments

ASTM SA 210-GrA1 (GrA1) boiler tube steel was selected as a candidate material in experimental work. This steel has a wide range of application in boilers, especially in

***Corresponding author: Ravindra Kumar,** Metallurgical and Materials Engineering Department, Indian Institute of Technology Roorkee, Roorkee 247667, India, E-mail: ravirs_2002@rediffmail.com
V. K. Tewari: E-mail: vinaykumartewari@gmail.com, **Satya Prakash:** E-mail: truthfmt@iitr.ernet.in, Metallurgical and Materials Engineering Department, Indian Institute of Technology Roorkee, Roorkee 247667, India

the construction of their water walls. The boiler tube (5 mm thickness × 33 mm diameter) was cut into approximate length of 150 mm each. Each tube was machined to obtained a single conventional V-groove, with 37.5^0 bevel angle, constant root gap 1 mm and root face 1 mm. Prior to welding the tube was thoroughly cleaned with brush and acetone so as to remove any oxide layer and dirt or grease adhering to the tube. Tubes were welded together by shielded metal arc welding (SMAW) using basic coated electrode E7018 and tungsten inert gas welding techniques using 99% pure argon gas with filler wire ER 70S-2 with constant arc current 95 A. Details of welding parameters are given in Table 1. The specimens, each measuring approximately $20 \times 15 \times 5\,mm^3$, were cut from the weldments portions. The specimens were polished with (220 grade) silicon carbide paper and emery paper (1/0, 2/0. 3/0, 4/0) then wheel polished before being to oxidize. The chemical composition of the base metal and the electrode/filler metal are given in Table 2.

High temperature oxidation test

Cyclic oxidation studies in air were conducted at 900°C temperature in the laboratory silicon carbide tube furnace for 50 cycles. Each cycle consisted of 1 h heating at 900°C followed by 20 min cooling at room temperature. The aim of cyclic loading is to create severe conditions for testing. The studies were performed for welded specimens for comparison. The specimens were mirror-polished before oxidation studies. During experimentation, the prepared specimen was kept in an alumina boat and the weight of the boat and specimens was measured. The alumina boats used for the studies were preheated at a constant temperature of 1200°C for 6–8 h, and it was assumed that their weight would remain constant during the course of high temperature cyclic oxidation study. Then the boat containing the specimen was inserted into the hot zone of the furnace set at a temperature of 900°C. The holding time in the furnace was 1 h in still air at an isothermal temperature of 900°C, after which the boat with specimen was taken out and cooled at ambient temperature for 20 min. Weight-change measurements were taken at the end of each cycle using an electronic balance (model 06120) with a sensitivity of 10^{-3} g. Any spalled scale was also included at the time of weighing to determine the total rate of corrosion. Efforts were made to formulate the kinetics of corrosion. After the oxidation studies, the exposed specimens were analysed by XRD and SEM-EDX analysis using Bruker AXS D-8 advance diffractometer (Germany) with Cu Kα radiation at the scan rate of 1°/min for 10° to 110° and Oxford (Model-6841), respectively. The oxidized specimens were then cut using Buehler's Precision Diamond saw (Low speed saw, 04006, USA make) across the cross section and mounted for the cross-sectional oxide scale thickness measurement.

Results and discussion

Visual observation and thermogravimetric data analysis in air

The weight gain plots of welded steels in air at 900°C is shown in Figure 1 and it can be seen in the plots the weight gain for both weldments was almost same in the initial number of cycles up to the 14th cycles then after gradually increased. It can be inferred from the plot that SMAW welded steel showed the maximum weight gain as compared to TIG welded steel. The amount of the spalled scale has also been incorporated in weight gain measurements. The colour of oxide scale during initial cycles for TIG weldment was blackish grey and turned light black after 34th cycle, cracks in the oxide scale had started appearing during 30th cycles. Where as in case of SMAW welded steel, the

Table 1: Welding process parameters.

Welding processes	Types of process	Arc voltage (Volts)	Arc current (Amp.)	Average welding speed (mm/min)	No. of pass	Average heat input (J/cm)	Electrode/ filler wire	Gas flow rate (l/min)	Electrode/filler wire size (mm)
TIG	Manual	12	95	46.93	4	14,575	AWS A5.18 ER 70 S-2	8	2.4
SMAW	Manual	22	95	140.47	2	8927	AWS A5.1 E7018	-	3.15

Table 2: Chemical composition (wt %) for Gr A1 boiler tube steel and electrode/filler wire used in present study.

Material	C	Mn	Si	S	P	Fe
Base metal	0.27	0.93	0.1	0.058	0.048	Balance
Electrode E7018	0.08	1.2	0.52	0.016	0.015	Balance
Filler wire ER70S-2	0.05	1.15	0.45	0.018	0.02	Balance

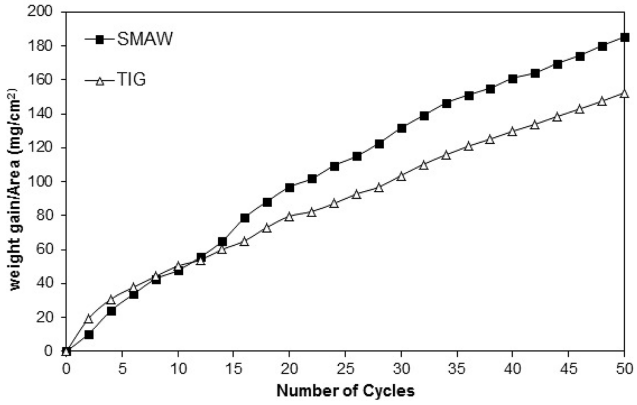

Figure 1: Weight gain plot for welded steels exposed to air at 900°C.

weld regions seen black in colour during 14th cycle and cracks seem after 27th cycle with little surface spallation. The width of cracks was comparatively more in case of SMAW welded steel than TIG welded. Oxide protrusions, blackish dark grey in colour have been observed through these cracks.

The behaviour for welded steel was almost parabolic with parabolic rate constants, K_p (10^{-8} $g^2 cm^{-4} s^{-1}$) is 20.365 (SMAW) and 13.074 (TIG) as shown in Figure 2. The total cumulative weight gain of these weldments is shown in Figure 3.

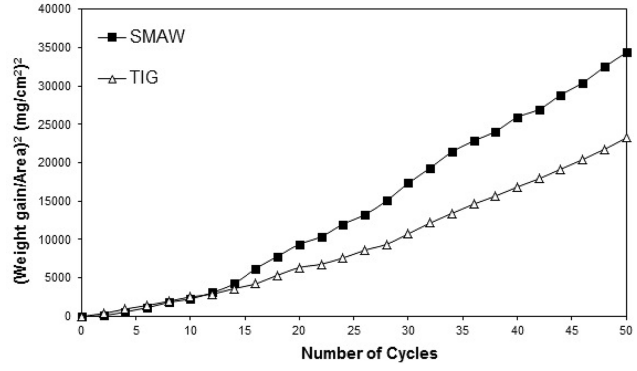

Figure 2: Weight gain square $(mg/cm^2)^2$ plot for welded steels exposed to air at 900°C.

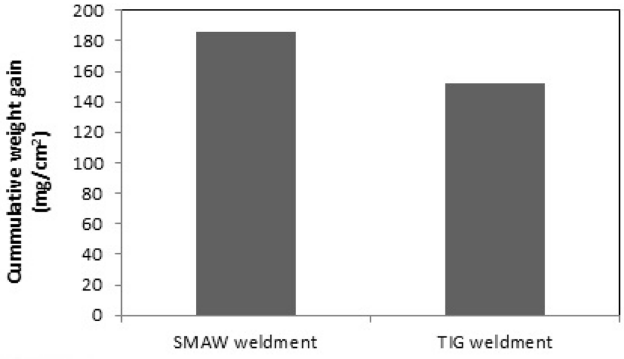

Figure 3: Cumulative weight gain of weldments.

Measurements of oxide scale thicknesses

The thickness of the oxide scale formed on the weldment (i.e. on weld metal and HAZ) measured from the BSEI, taken along the cross-section of the mounted specimens, images for all the specimens are shown in Figure 4. The average scale thickness values measured for weld region of SMAW and TIG weldment in steels are 1.110 mm and 0.704 mm, respectively. Whereas average scale thickness measured for HAZ region of SMAW and TIG weldment are 1.196 mm and 0.843 mm, respectively. Minimum scale thickness is indicated by TIG weld metal. There were the cracks in the scale of HAZ of SMAW. The cross sectional image for the oxide scale of HAZ of SMAW weldment indicates cracks right through scale, whereas the oxide scale debonding at metal/scale interface is evident from Figure 4 (b), (c) & (d) for HAZ of SMAW and TIG welded steels, respectively.

X-ray diffraction studies

In the given environment, both the weldment had Fe_2O_3 as the main constituent of scale, as shown in Figure 5. High intensity peaks were observed in case of SMAW welded steel than that of TIG welded.

Surface morphology of the scales

SEM photographs showing surface morphology of the welded steel after cyclic oxidation at 900°C in air for 50 h are shown in Figure 6. It was observed that the scale containing distorted grains consists of mainly iron oxide. SMAW welded steel shows more oxidation along boundaries of globules. The top scale contains larger amount of

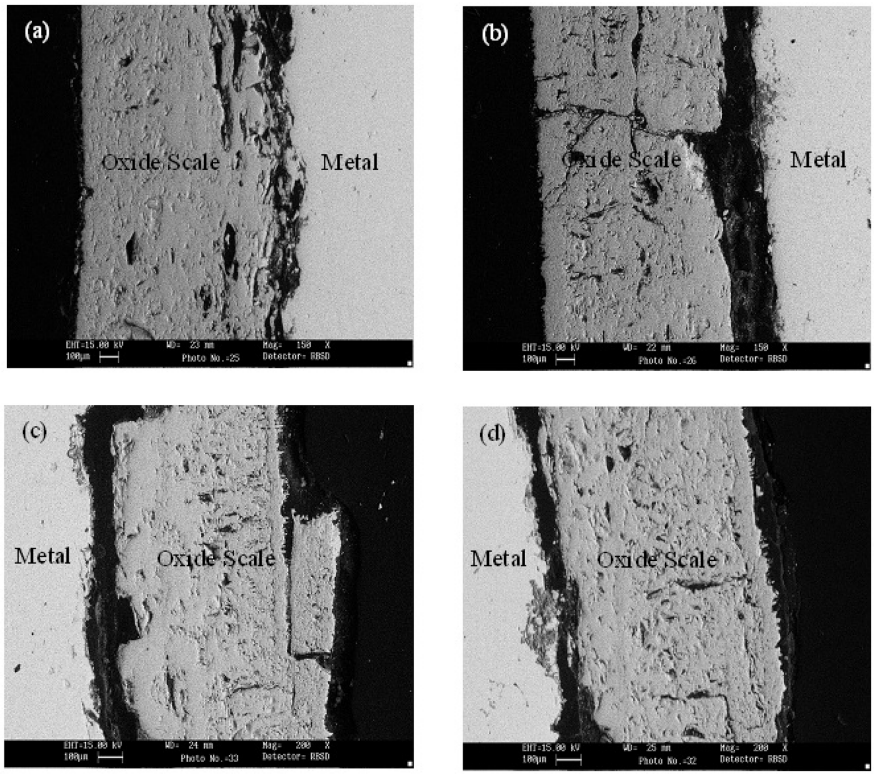

Figure 4: SEM back scattered image of the cross section of welded steels after cyclic oxidation in air at 900°C for 50 cycles (a) weld metal (SMAW) (b) HAZ (SMAW) (c) weld metal (TIG) (d) HAZ (TIG).

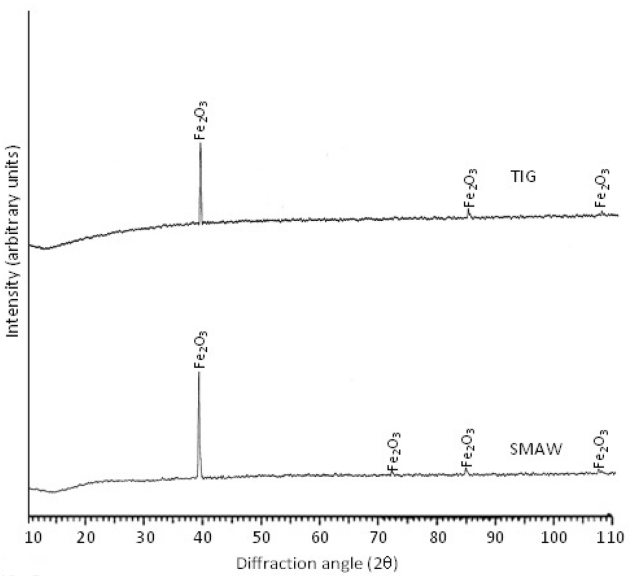

Figure 5: X-ray diffraction profiles for welded GrA1 steel exposed to air at 900°C for 50 cycles.

iron oxide (99.44%) as compared to boundary region having 99.11% iron oxide. Whereas the oxide scale of HAZ region consists of mainly iron oxide (99.01%) with small amount of MnO (0.65%) at Point 2 in Figure 6(b). The weld region of TIG weldment indicates a scale rich in Fe_2O_3 (99.60%) as revealed by EDX. Oxide protrusions from inside consisting mainly of Fe_2O_3 (99.83%) indicated point 1 Figure 6 (c). The upper oxide scale on HAZ region consists of iron oxide Fe_2O_3 and SiO_2 (2.56%) at point 2, whereas the inner scale (Point 1) consists of 99.20% Fe_2O_3 with small amount of MnO Figure 6 (d).

From Figure 2 it can be inferred that both weldments shows same weight gain during initial number of cycles up to 14th but subsequently increase in weight is gradual and almost follow parabolic oxidation rate law. The oxidation resistance in air was more of TIG welded steel as compared to SMAW. The XRD analysis revealed mainly the presence of Fe_2O_3 in the scale of both the weldments with high intensity peaks in case of SMAW welded steel. Fe_2O_3 might be formed due to the interdiffusion of oxygen and interaction with the metal surface. Fe_2O_3 formation has also been reported as the main oxide in base steel by Sidhu and Prakash [12]. In terms of scale thickness measurements the weld region and HAZ of SMAW welded specimen shows more oxidation than that of weld and HAZ regions of TIG welded, the reason was the development of internal oxidation, more cracks and spallation of

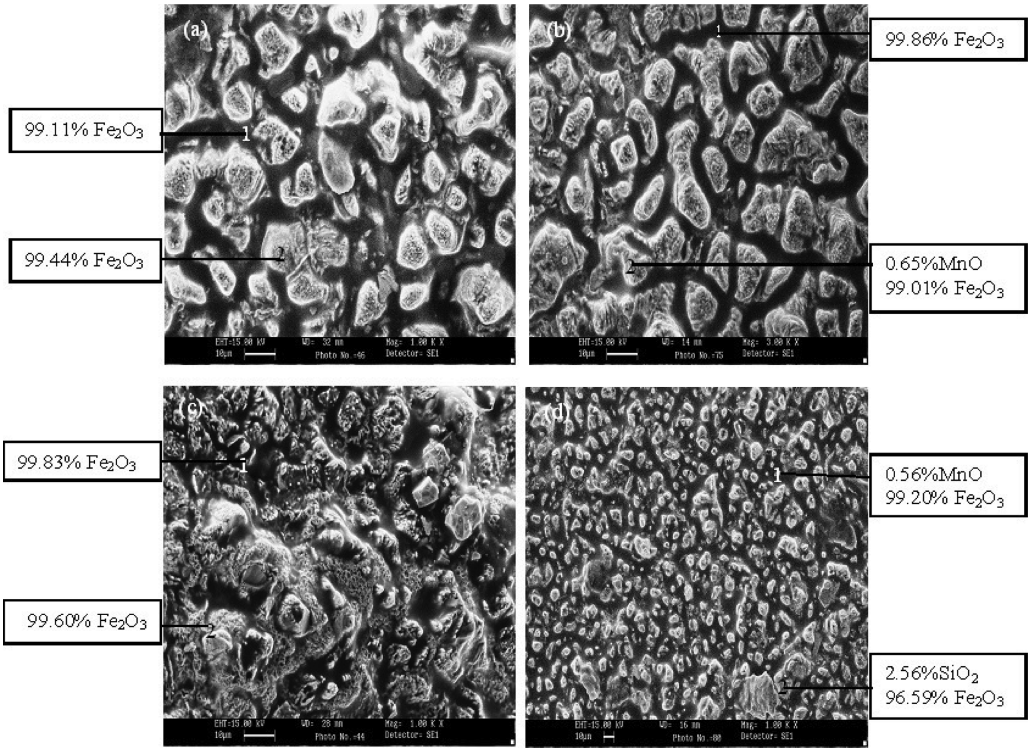

Figure 6: Surface morphology and EDX analysis of the scale on welded GrA1 steels exposed to air at 900°C (a) weld metal (SMAW) (b) HAZ (SMAW) (c) weld metal (TIG) (d) HAZ (TIG).

oxide scale during oxidation run. Spalling of the oxide scale was due to different values of thermal expansion coefficients of the metal and oxides as discussed by Young [13]. The result of XRD was in accordance with the surface EDX analysis. In case of SMAW welded steel, EDX analysis revealed the top and inner scale was richer in iron oxide of weld and HAZ regions, whereas in case of HAZ region of TIG welded steel Si was observed in small amount with main iron oxide. The presence of Si in the oxide of HAZ region of TIG weldment may result of less oxidation in the given environment.

Conclusions

Based on thermogravimetric studies under cyclic condition the following conclusions have been drawn:

Fe_2O_3 has been found as main oxide in the welded GrA1 steels as revealed by XRD, and EDS analysis. SMAW welded steel showed the more weight gain than that of TIG welded and it was due to the formation of internal oxidation, more cracks and spallation of oxide scale, and a thicker oxide scale was found on HAZ and weld region (as confirmed by oxide scale thicknesses measurements BSEI).

Both the weldments in GrA1 steel follows the parabolic rate law in air at 900°C. Maximum cracking was observed in the case of SMAW weldment during air oxidation which provides the easy diffusion path for corrosive elements, whereas it was least in TIG weldment.

References

[1] K. Laha, K.B.S. Rao and S.L. Mannan, Mat. Sci. Eng., A129 (1990) 183–195.
[2] American Society of Mechanical Engineers, "ASME Boiler and Pressure Vessel Code," Code Case N-47, ASME, Fairfield, NY (1986).
[3] R.K.S. Raman, Metall. Mat. Trans. A, 26 (1995) 1847–1858.
[4] R.K.S. Raman and J.B. Gnanamoorthy, Corrosion Sci., 34 (1993) 1275–1288.
[5] J. Pilling and N. Ridley, Metall. Trans. A., 13 (1982) 557–563.
[6] P. Roy and T. Lauritzen, Welding J. Research Suppl., 65 (1986) 45s–52s.
[7] H.B. Cary, Modern Welding Technology, prentice Hall, Inc,, Englewood cliffs, NJ (1979).
[8] R.K.S. Raman, Metall. Mat. Trans. A, 30 (1999) 2103–2113.
[9] S.E. Sadique, A.H. Mollah, M.S. Islam, M.M. Ali, M.H.H. Megat and S. Basri, Oxid. Metals, 54 (2000) 385–400.

[10] R. Kumar, V.K. Tewari and S. Prakash, Oxid. Metals, 86 (2016) 89–98.
[11] R. Kumar, V.K. Tewari and S. Prakash, J. Alloys Comp., 479 (2009) 432–435.
[12] B.S. Sidhu and S. Prakash, Surf. Coat. Techn., 166 (2003) 89–100.
[13] D.J. Young, High Temperature Oxidation and Corrosion of Metals, NY: Elsevier Publisher (2008).